PREPARATION, CHARACTERIZATION AND EVALUATION OF *Irvingia gabonensis* SEED SHELL CARBON FOR SORPTIVE REMOVAL OF PHOSPHATE IONS IN WASTEWATER

P. I. Utange[1]*, R. A. Wuana[2] and I. S. Eneji[2]
[1]Department of Chemistry, Benue State University, Makurdi, Nigeria
[2]Department of Chemistry/Centre for Agrochemical Technology and Environmental Research,
Federal University of Agriculture, Makurdi, Nigeria
*Corresponding author: putange@bsum.edu.ng

Abstract: The sorptive removal of phosphate ions in wastewater from an advanced multipurpose chemistry laboratory was carried out using two activated carbon adsorbents of particle size 150 μm (CIG150) and 300 μm (CIG300) prepared from seed shells of *Irvingia gabonensis* and a commercial activated carbon (CAC). The physicochemical attributes of CIG150, CIG300 and CAC were found to be pH_{pzc}: 3.0 − 7.1; ash content (%): 3.04 − 11.5; bulk density (kg/m^3): 173 − 479; attrition (%):12.9 − 19.7; iodine number ($\times10^{-3}$ mol/g): 0.966 − 1.486; surface area (m^2/g): 186.09 − 286.26; and surface charge (mmole H^+ eq/g) − NaOH: 0.890 − 1.214. Optimum adsorption capacity was achieved at pH 7 for all the adsorbents. Langmuir isotherm ranged as: maximum adsorption capacity, Q_m (mg/g) for the study were 298 K: 0.7492 − 0.9329; 303 K: 0.7820 − 0.9444; 308 K: 0.8114 − 0.9944. The thermodynamic quantities indicated spontaneous, exothermic and physical adsorption process for the uptake of phosphate ions onto the adsorbents. The Weber-Morris intra-particle kinetic model better explained the adsorption process. All the adsorbents exhibited good efficiency for the uptake of phosphate ions (64.15–75.11%) and the potency was in the order of CAC>CIG300>CIG150.

Keywords: Activated carbon, adsorption, *Irvingia gabonensis,* isotherm, kinetics, wastewater

Introduction

The disposal of wastes pose significant challenges the world over, due to the perception of risk to human health and the environment (Alghanmi *et al.*, 2015). It is however, a common practice in developing nations that laboratory wastewater is drained down the sink into septic tank – soakaway systems without prior pre-treatment. The "septic tank – soakaway" system can be likened to a sanitary landfill in that while a septic tank – soakaway system houses liquid waste, a landfill houses solid waste; and a number of environmental and health concerns have been associated with landfills (Vrijheid, 2000; Olorunfemi, 2009; Akinjare *et al*., 2011a; Olorunfemi, 2011; Aderemi and Falade, 2012; Oladapo *et al*., 2013). Similar concerns can be likened to septic tank – soakaway systems, resulting to negative impacts such as groundwater contamination (Akinjare *et al*., 2011b).

There are three (3) mandatory tests under building regulations that must be undertaken to determine whether or not, to construct a sewage soakaway. These include groundwater source protection zone test, the trial site assessment hole test and percolation test in that order (WTEL, 2016). These mandatory tests are aimed at ensuring that groundwater designated for use as drinking water source is prevented from contamination by effluents from the soakaway. It is therefore important that a soakaway system does not provide a pathway to connect a contamination source to a groundwater target thereby forming the source-pathway-target (SPT) chain. Despite the potential for pollution and unsatisfactory performance of many systems, septic tank-soil absorption systems continue to provide a valuable domestic waste treatment alternative especially where housing density cannot economically justify sewers and treatment plants.

Septic systems have performed a vital function of environmental sanitation, particularly in rural and sparsely developed suburban areas. However, some estimates indicate that less than one-half of all systems in use today perform satisfactorily for the entire design life of fifteen to twenty years. Many public health authorities opine that conventional septic systems are suitable only where population density is strictly limited and soil conditions are suitable for effective absorption. Otherwise these systems may contaminate ground and surface waters and result to sanitary nuisances and health hazards (Zhang *et al.,* 2013).

Because of improper design, improper construction or improper maintenance or a combination of these, a significant percentage of septic systems fail within their design life. Soils in many areas, perhaps in much as one-half (in the United States for instance) are not suitable for conventional septic tank-soil absorption systems. Septic tank systems are common sources of water, especially ground water contamination. In Nigeria, the mandatory tests required to be carried out before embarking on the construction of septic tank – soakaway systems are often ignored, hence the aim of preventing groundwater designated for use as drinking water source from contamination is defeated. In general, subsurface sewage disposal systems are the largest sources of wastewater to the ground, and are the most frequently reported causes of groundwater contamination (Wuana *et al.,* 2010).

Industrial development, urbanization and uncontrolled agricultural practices have resulted in severe environmental problems (Ameh *et al.*, 2012). Contamination is increasing in various sites including residential areas near industrial complexes and reservoirs of drinking water which have enormous impact on the quality of groundwater. The solubility and extent of these contaminants in the subsurface system is influenced by the chemistry of the groundwater, like pH, redox potential, chelation, etc. (Alghanmi *et al*., 2015; Khalil *et al.*, 2015).

Hanchar (1991) pointed out that phosphate, sulphate, chloride, nitrate ions are commonly found in groundwater, but when present at elevated concentrations indicate influence of human activity. A number of environmental problems have been associated with the presence of phosphate ions in water. Research has shown that, phosphate can reach groundwater and move down-gradient in the septic plume and that migration exceeds ten (10) metres of investigated plumes. Phosphate may be a concern in poorly buffered systems if the pH within the plume drops below 6.0. Although water quality of individual septic systems are similar, groundwater quality within an aquifer will continue to change until plumes from individual systems stabilize. Eutrophication, for example, continues to be a worldwide environmental problem caused

FUW Trends in Science & Technology Journal, www.ftstjournal.com
e-ISSN: 24085162; p-ISSN: 20485170; April, 2021: Vol. 6 No. 1 pp. 024 – 037

024

by excessive nutrient inputs, particularly of phosphorus (Stoica *et al.*, 1999; Agrawal *et al.*, 2015).

It is also reported that eutrophication has seriously affected biodiversity, vegetation development and terrestrialization in fens in addition to the interaction effect with toxicity. As a consequence, many characteristic plant species have disappeared and have been out competed by a few fast growing species. Apart from the decrease in biodiversity, the characteristic plant species that disappeared often served as ecosystem engineers: key species that can colonize the water layer, form floating mass and initiate terrestrialization processes in fens. It has also been shown that in the absence of these species, there will be no peat formation but net peat degradation, especially because eutrophication will increase nutrient concentrations in the organic matter (Chislock *et al.*, 2013; Geurts *et al.*, 2009).

Several techniques have been adopted in the removal of contaminants from wastewater namely chemical precipitation, ion exchange, adsorption, membrane filtration, coagulation and flocculation, floatation and electrochemical treatment (Fu and Wang, 2011; Zhang *et al.*, 2014; Al-Qahtani, 2016). All these techniques employed have their inherent advantages and limitations and of all, ion exchange, adsorption and membrane filtration appear to be the most widely used with adsorption recognized as an effective and economic method for low concentration contaminants in wastewater treatment due to its low initial cost, low energy requirements, simplicity of design and possibility of regeneration (Namasivayam and Sangeetha, 2005; Fu and Wang, 2011). Biosorption, which involves active and non-active uptake by biomass, is a good alternative to traditional processes. The wide use of biopolymers in sorption studies is not unconnected to the fact that, they are widely available and cheap. This in addition to the risk to human health and environment, stimulates the interest in this study exploring the use or otherwise of seed shells of *Irvingia gabonensis* as an adsorbent for the removal of phosphate ions in wastewater.

In consideration of the health – based targets which are measurable health outcomes, water quality, performance or specified technology objectives established based on the judgement of safety and risk assessments of water borne hazards (WHO, 2011), phosphates constitute a major contaminant in water among other anions. In light of the above, this study demonstrates the use of available environmentally friendly and cheap agricultural waste from seed shells of *I. gabonensis* as a potential source of adsorbent, to be used in solving wastewater treatment problem.

Materials and Methods
Preparation of adsorbent from I. gabonensis seed shells
Irvingia gabonensis seed shells were collected from Shangev in Kwande Local Government Area of Benue State. The precursor was pulverized using mortar/pestle and then hammer mill, and the resulting powder sieved using a graded sieve. Two portions of the sieved material of particle size 150 and 300 µm were activated and pyrolyzed according to the method reported by Okiemen *et al.* (2007). The resulting carbon was rinsed with distilled water to remove ash, air-dried, sieved again using graded sieve. The 150 and 300 µm fractions were respectively labelled as CIG150 and CIG300 carbonized adsorbent.

Physicochemical characterisation of adsorbents
The adsorbent was characterised in terms of the following properties: pH point of zero charge (pH_{pzc}), ash content, bulk density, attrition, iodine adsorption number/adsorbent surface area, titratable surface charge, Fourier transform infrared spectroscopy (FT-IR) and scanning electron microscope (SEM).

pH_{pzc} determination: The pH point of zero charge (pH_{pzc}) of the adsorbent was determined using salt addition method. In this method, 50 mL of 0.01 $molL^{-1}$ NaCl solution was measured into ten (10) Erlenmeyer flasks. The pH of the solution in the flasks were adjusted to values of 2, 3, 4, 5, 6, 7, 8, 9, 10, and 11 by adding 0.1 $molL^{-1}$ HCl or 0.1 $molL^{-1}$ NaOH solution. Then 0.5 g of the adsorbent was added and agitated on a shaker for 1 hour and then allowed to settle for 48 h to reach equilibrium at prevailing temperature. The pH of the solution was then determined for the adsorbent. A graph of initial pH (pH_o) versus the differences between the initial and final pH values (ΔpH) was plotted. The pH_{pzc} was taken as the point where $\Delta pH=0$ (Abia and Asuquo, 2007; Cardenas-Peña *et al.*, 2012).

Ash content: A clean empty crucible was preheated in a furnace at 500ºC for 1 h; it was then cooled in a desiccator and weighed (W_1). Then 2.0 g of the adsorbent was weighed into the preheated crucible (W_2). The crucible and its content was placed in the muffle furnace and the temperature was raised to 550ºC for four hours, allowed to cool to 200ºC and finally cooled in a desiccator before weighing (W_3). The whole process was repeated twice and the average was recorded (Okieimen *et al.*, 2007). Ash content was expressed using the relationship:

$$\% \text{ Ash content} = \frac{w_3 - w_1}{w_2 - w_1} \times 100 \tag{1}$$

Bulk density determination: The bulk density of the samples was determined according to the method described by Dada *et al.* (2012). A 10 mL measuring cylinder was dried and pre-weighed (w_1), then packed with the sample, levelled and weighed (w_2). The volume (v) of the packed material was then read and bulk density determined according to the equation:

$$\text{Bulk density} = \frac{w_2 - w_1}{v} \tag{2}$$

The procedure was repeated twice and the mean bulk density calculated.

Determination of attrition: The percentage attrition of the samples was determined according to the method described by Hassan *et al.* (2012) with little modification. A 1.0 g portion of the adsorbent was added to 100 mL of acetate buffer (0.07 M sodium acetate and 0.03 M acetic acid, pH 4.8) in a 250 mL beaker. The mixture was stirred for 24 h at 500 rpm. The mixture was then filtered and washed with 250 mL of deionized water. After washing, the retained sample was transferred to a pre-weighed dish and dried at 90ºC under vacuum for 24 h. The sample was then cooled in a desiccator and weighed. The procedure was carried out in triplicate and mean percentage attrition obtained. The percentage attrition was calculated according to the equation:

$$\text{Attrition}(\%) = \frac{\text{Initial weight (g) - Final weight (g)}}{\text{Initial weight (g)}} \times 100 \tag{3}$$

Iodine adsorption number/adsorbent's surface area: The determination of iodine adsorption number/adsorbent's surface area was adopted from Okiemen *et al.* (2007) without modification. A 0.5 g portion of the adsorbent was added to 25 mL of the standard iodine solution. The mixture was stirred vigorously for 10 minutes and filtered. A 20 mL aliquot of the iodine filtrate was back-titrated against a standard thiosulphate. This procedure was repeated twice and average of the iodine number, n_{I_2} (i.e., amount in moles of

FUW Trends in Science & Technology Journal, www.ftstjournal.com
e-ISSN: 24085162; p-ISSN: 20485170; April, 2021; Vol. 6 No. 1 pp. 024 – 037

025

iodine adsorbed per g adsorbent) was calculated using equation:

$$n_{I_2}(\text{mol.g}^{-1}) = \frac{C_{S_2O_3^{2-}}(V_b - V_s)}{2 \times 10^3 m_a} \qquad (4)$$

While the adsorbent surface area, A (m^2g^{-1}) was calculated using the equation described by Wuana *et al*. (2015) presented thus:

$$A\,(\text{m}^2.\text{g}) = N_o \left[\frac{C_{S_2O_3^{2-}}(V_b - V_s)}{2 \times 10^3 m_a} \right] \sigma_{I_2} \qquad (5)$$

Where $C_{S_2O_3^{2-}}$ is the concentration of the thiosulphate (mol L^{-1}); V_b and V_s are respectively the titre values of the blank and adsorbent-treated iodine solutions (mL); m_a is mass of the adsorbent used (0.5 g); N_o is the Avogadro's number; and σ_{I_2} is the cross-sectional area of an iodine molecule (m^2), given as 3.2 x 10^{-19} m^2.

Titratable surface charge: The modified Boehm titrimetric method described by Paul *et al*. (2016) was adopted to determine the total negative surface charge. A suspension of 1.0 g of the adsorbent in 50 mL of 0.1 M NaOH was stirred in a closed vessel for approximately 20 to 24 h. The slurry was filtered and a 10 mL aliquot was added to 15 mL of standard 0.1 M HCl solution. The HCl neutralized the unreacted base. The solution was then back titrated with standard 0.1 M NaOH, the volume of NaOH required to neutralize the sample was converted to titratable negative surface charge. Results were expressed in mmoles H^+ ions neutralized by excess OH^- ions per g of adsorbent.

Fourier transform infrared (FTIR) spectroscopy: A small portion of the adsorbents was taken and each ground in a mortar until the sample had a glossy appearance, then about 2 – 6 mg of KBr was added to the sample and ground until a homogeneous blend was obtained. The scan was run using the FT-IR spectrometer

Scanning electron microscope (SEM): The surface morphology of the adsorbents was characterized by Scanning Electron Microscope (SEM). The scanning electron micrographs for all the adsorbents were obtained at 500x magnification and at bright field of 15 kV.

Collection of wastewater, identification and quantification of cations and anions

A 300-L plastic container was placed in the Multipurpose Chemistry Laboratory of Benue State University, Makurdi between April and July, 2018. All reaction mixtures and laboratory washings were dispensed into the plastic container instead of draining same down the sink into the septic tank – soak away system for the purpose of this study. This mixture represents sample to be collected from the septic tank – soak away system.

The cations and anions present in the wastewater collected were identified and the concentration of phosphate ions was estimated before and after contact with the adsorbents.

Identification of cations and anions: The cations and anions present in the wastewater water collected were identified using standard tests for lead, cadmium, copper, manganese, nickel, zinc, iron, mercury, sulphate, carbonate, nitrate and phosphate ions prior to adsorption studies (Gusau, 1992; Harvey, 2000; Yoder, 2016).

Determination of phosphate ions/formation of calibration curve: The molybdenum blue method described by Utange *et al*. (2015) was modified for the spectrophotometric determination of phosphate ions. A solution containing 1000

mg PO_4^{3-}/L was prepared by dissolving 1.4329 g dry KH_2PO_4 in 1 L of distilled water. A working standard was prepared by diluting 10 mL of the stock solution to 100 mL, containing 100 mg PO_4^{3-}/L. Standard solutions containing 3, 6, 9, 12 and 15 mg PO_4^{3-}/L were prepared by diluting 3.0, 6.0, 9.0, 12.0 and 15.0 mL of the working standard to 100 mL, respectively. The mixed reagent for colour development was prepared by thorough mixing of 125 mL of 5 N sulphuric acid and 37.5 mL of ammonium molybdate (20 g/500 mL), followed by addition of 75 mL of ascorbic acid solution (0.1 M) and 12.5 mL of potassium antimonyl tartrate solution (1 mg Sb/mL). This reagent was prepared as required as it does not keep for more than 24 h.

A 20 mL aliquot of the sample/standard was pipetted into a 25 mL calibrated flask and 4 mL of the mixed reagent added. The contents was diluted to volume with distilled water, and mixed well. After 10 minutes, the absorbance of the solution was measured at 690 nm using a standard quartz cell in a UV-Visible spectrophotometer. The reagent blank was prepared in the same manner using freshly distilled water to zero the spectrophotometer. The calibration curve was prepared from the results of the standard solutions as presented in Fig. 1.
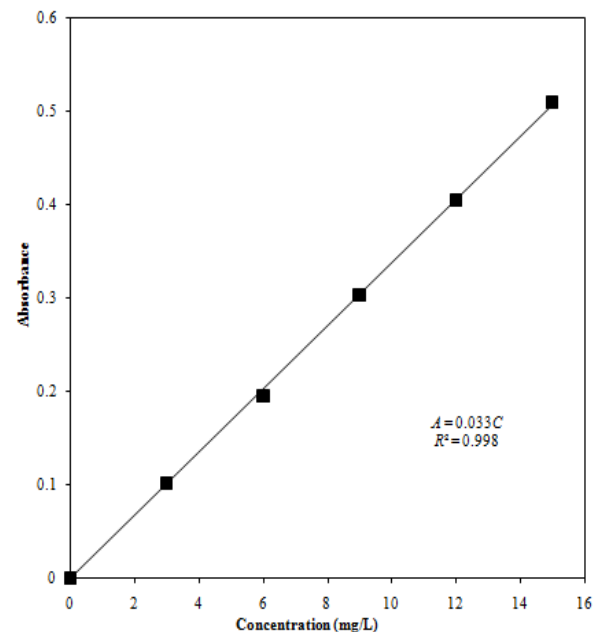

Fig. 1: Calibration curve for determination of phosphate ions in wastewater

Adsorption experiments
The adsorption experiments were carried out in batch mode (Oboh *et al.,* 2013) and were conducted by measuring 100 mL of wastewater into a 250 mL conical flask. To the wastewater, 1.0 g of the adsorbent (synthesized and commercial) was added. The flask containing adsorbent and wastewater was placed on a shaker or water bath for contact. Separation of the loaded adsorbent and wastewater was carried out by filtration using Whatman filter paper. Batch adsorption studies were conducted according to the method described by (Wuana *et al*., 2015) with little modifications.

Effect of initial pH: The effect of solution pH on the adsorption of phosphate ions was studied by treatment of aliquots of the wastewater (whose pH were adjusted to values (±0.1) of 3, 5, 7, 9 and 11) with 1.0 g of the adsorbents for 4 h at laboratory temperature (298 ±3 K). The residual concentrations of phosphate ions were determined thereafter.

FUW Trends in Science & Technology Journal, www.ftstjournal.com
e-ISSN: 24085162; p-ISSN: 20485170; April, 2021: Vol. 6 No. 1 pp. 024 – 037

026

Effect of adsorbent dosage: A 0.5, 1.0, 1.5, 2.0 and 2.5 g portions of each adsorbent was contacted with the wastewater for 4 h at three different temperatures (K); 298, 303 and 308 in a thermostatic water bath and the residual concentration of phosphate ions determined.

Effect of contact time: Aliquots of the wastewater were separately contacted with 1.0 g of each adsorbents for 10, 30, 60, 120, 180, 240 min, at 298 K in a thermostatic water bath. The experiment was repeated at temperatures (K) of 303 and 308. The residual concentrations of phosphate ions in the mixtures were determined.

Data treatment
The amount of phosphate ions adsorbed were calculated using the mass balance equation described by Itodo and Itodo (2010) as presented in Equation (6) while percentage removal was calculated by Equation (7);

$$q_e = \frac{(C_o - C_e)V}{m} \qquad (6)$$

$$\% \text{ Removal} = \frac{C_o - C_e}{C_o} \times 100 \qquad (7)$$

Where C_o and C_e are the initial and residual phosphate ions concentrations (mg L^{-1}), respectively; V is the aliquot of wastewater used in L; and m is the mass (g) of adsorbent used for a particular batch treatment.

The data obtained from adsorption experiments were modelled according to the linear forms of Langmuir (Equation 8), Freundlich (Equation 9), Temkin (Equation 10) and Dubinin-Radushkevich isotherms (Equation 11). A dimensionless equilibrium parameter called separation factor *[R_L]* (Equation 12) was used to study the applicability of Langmuir isotherm. Modelling of sorption kinetics was also carried out according to the linearized forms of Lagergren pseudo-first order (Equation 13), Blanchard pseudo-second order (Equation 14) and Weber-Morris intra-particle diffusion models (Equation 15).

$$\frac{C_e}{q_e} = \frac{1}{q_m K_L} + \frac{C_e}{q_m} \qquad (8)$$

$$\log q_e = \log K_f + \frac{1}{n} \log C_e \qquad (9)$$

$$q_e = B \ln A_T + B \ln C_e \qquad (10)$$

$$\ln q_e = \ln q_s - K_{DR} \varepsilon^2 \qquad (11)$$

$$R_L = \frac{1}{1 + (1 + K_L C_o)} \qquad (12)$$

$$\ln(q_e - q_t) = \ln q_e - k_1 t \qquad (13)$$

$$\frac{t}{q_t} = \frac{1}{k_2 q_e^2} + \frac{1}{q_e} t \qquad (14)$$

$$q_t = k_{id} \sqrt{t} + C \qquad (15)$$

The adsorption data obtained from the synthesized and commercial adsorbents were presented using descriptive statistics in tables or graphs.

Results and Discussion
Physicochemical properties of adsorbents from Irvingia gabonensis seed shells and a commercial product
Some physicochemical properties (pH$_{pzc}$, ash content, bulk density, attrition, iodine number, surface area, surface charge, FT-IR and SEM) of activated carbon of particle size 150 μm (CIG150) and 300 μm (CIG300) derived from seed shells of *I. gabonensis* and those of a commercial activated carbon (CAC) are recorded in Table 1. The plots for the determination of pH$_{pzc}$ were presented in Fig. 2. The FT-IR spectra of the adsorbents used are presented in Fig. 3; while the FT-IR spectral bands are summarised in Table 2 and the surface characteristics or scanning electron micrographs of *I. gabonensis* seed shells carbon (CIG150 = 150 μm; CIG300 = 300 μm Particle Size) and commercial activated carbon (CAC) are as presented in Fig. 4.
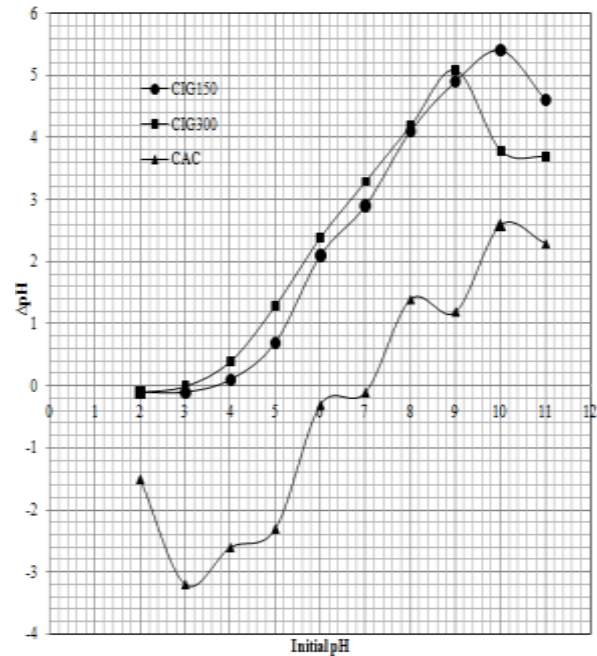

Fig. 2: Plots for the determination of pH$_{pzc}$

Table 1: Selected physicochemical attributes of *I. gabonensis* seed shell carbon in comparison with commercial activated carbon†

Attribute	CIG150	CIG300	CAC
pH$_{pzc}$	3.7	3.0	7.1
Ash content (%)	3.04 ± 0.14	4.32 ± 0.20	11.52±1.41
Bulk density (kg/m³)	173±21	269±2	479±17
Attrition (%)	19.71±1.26	14.65±2.07	12.91±0.47
Iodine number (mg/g)	245.17	320.54	377.14
Iodine number (×10^{-3}mol/g)	0.966	1.263	1.486
Surface area (m²/g)	186.09	243.30	286.26
Surface charge (mmol H$^+$eq/g)-NaOH	0.890	1.097	1.214

†CIG150 = carbonized I. gabonensis seed shells (particle size of 150 μm); CIG300 = carbonized I. gabonensis seed shells (adsorbent particle size of 300 μm); CAC = commercial activated carbon

FUW Trends in Science & Technology Journal, www.ftstjournal.com
e-ISSN: 24085162; p-ISSN: 20485170; April, 2021: Vol. 6 No. 1 pp. 024 – 037

027

Sorptive Removal of Phosphate Ions in Wastewater Using I. gabonensis Adsorbent

Table 2: Langmuir isotherm parameters for adsorption of selected phosphate ions on carbonized *Irvingia gabonensis* seed shells (CIG150 and CIG300) and commercial adsorbent (CAC) at different temperatures

Adsorbent	Model	298K	303K	308K
CIG150	Q_m (mg.g^{-1})	0.7492	0.7820	0.8114
	K_L (L.mg^{-1})	1.7347	1.6190	1.4676
	K_L ($\times 10^5$ L.mol^{-1})	1.6475	1.5376	1.3938
	R^2	0.9999	0.9991	0.9997
	R_L	0.0113	0,0121	0.0133
CIG300	Q_m (mg.g^{-1})	0.8179	0.8447	0.9061
	K_L (L.mg^{-1})	1.6578	1.2564	0.9475
	K_L ($\times 10^5$ L.mol^{-1})	1.5744	1.1932	0.8998
	R^2	0.9992	0.9982	0.9989
	R_L	0.0118	0.0154	0.0203
CAC	Q_m (mg.g^{-1})	0.9329	0.9444	0.9944
	K_L (L.mg^{-1})	0.7373	0.6941	0.6033
	K_L ($\times 10^4$ L.mol^{-1})	7.0023	6.5923	5.7294
	R^2	0.9991	0.9896	0.9960
	R_L	0.0257	0.0272	0.0311

pH$_{pzc}$: From the results in Table 1, the pH$_{pzc}$ for CIG150 and CIG300 were 3.7 and 3.0, respectively. These observed values may be attributed to the fact that, even though the same material and activating reagent were used in preparing the adsorbents, pore size could have been responsible for the difference in the pH$_{pzc}$. The results of CIG300 for instance thus indicate that, at solution pH values greater than 3 (pH>3), the adsorption of positively charged species would be more favourable using the adsorbent, whereas at solution pH values less than 3 (pH<3), the adsorption of negatively charged species would be more favourable using the adsorbent. The same adsorption pattern would apply for CIG150 and CAC with a pH$_{pzc}$ values of 3.7 and 7.1 (Cardenas-Peña *et al.*, 2012).

Ash content: The results from Table 1 shows that CIG150, CIG300 and CAC respectively have ash content of 3.04±0.14, 4.32±0.20 and 11.52±1.41% indicating high presence of inorganic matter in the adsorbents used. The results of this study are comparable to those presented by Aminu *et al.* (2010) on granulated activated carbon from groundnut shells but lower than 18.39 % reported by Ye *et al.* (2012) for modified rice husk. The ash content of the prepared adsorbents met the Indonesian National Standard of maximum limit of 10% set for activated carbon as reported by Maulina and Iriansyah (2018). The high ash content of CAC could be attributed to its high resistance to pyrolysis as it took longer time with addition of acids to get the ash that was obtained; maybe there may have been incomplete pyrolysis. The high resistance to pyrolysis indicates that the adsorbent could be regenerated for re-use.

Bulk density: The high bulk density values of CIG150, CIG300 and CAC as presented in Table 1 are respectively 173±21, 269±2 and 479±17 indicating that they would be good adsorbents in the order of CAC>CIG300>CIG150. These values are comparable to those reported by Dada *et al.* (2012) [0.386 g/cm^3≡ 386 kg/m^3 for phosphoric acid modified rice husk], Fasoto *et al.* (2014) [0.235, 0.254 and 0.269 g/cm^3≡ 235, 254 and 269 kg/m^3 for activated sugarcane bagasse, modified sugarcane bagasse and unmodified sugarcane bagasse, respectively] and Wuana *et al.* (2016) [182.4 and 235.8 kg/m^3 for ammonium chloride treated *Moringa oleifera* pod husk and carbonized ammonium chloride treated *Moringa oleifera* pod husk respectively] and lower than that reported by Mallikarjun and Mise, (2012) [1,173.3 kg/m^3 for clay soil], and Das *et al.* (2014) [1.351 g/cm^3≡ 1,351 kg/m^3 for alluvial soils].

Attrition: From the results in Table 1, CIG150, CIG300 and CAC showed 19.71±1.26 %, 14.65±2.07 % and 12.91±0.47 % attrition respectively, indicating that resistance to abrasion was in the order of CAC>CIG300>CIG150. These values are relatively high compared to those reported by Wuana *et al.* (2015) on activated carbon derived from chemically activated *Moringa oleifera* pod (AMOP) and carbonized *Moringa oleifera* pod (CMOP) which showed 9.39 and 12.55 %, respectively.

Iodine adsorption number: Values of iodine adsorption number for CIG150, CIG300 and CAC as presented in Table 1 are respectively 245.17, 320.54 mg/ and 377.14 mg/g indicating high values compared to those reported by Wuana *et al.* (2015) for chemically activated and carbonized *Moringa oleifera* pods (256.40 and 310.60 mg/g). Adsorbents which have high iodine adsorption numbers tend to be better in the removal of small-sized contaminants (Ameh *et al.*, 2012; Wuana *et al.*, 2015).

Surface area: The surface areas (m^2/g) of CIG150, CIG300 and CAC were respectively 186.09, 243.30 and 286.26 as presented in Table 1. Activated carbons are generally known to have large surface area. The values obtained are comparable to those reported by Wuana *et al.* (2015) for chemically activated and carbonized *Moringa oleifera* pods (182.41 and 235.79 m^2/g) which shows that all adsorbents used could have high adsorption capacity.

Surface charge: The surface charge for the adsorbents is in the order of CAC>CIG300>CIG150 i.e. 1.214>1.097>0.890 indicating that the adsorbents are good for adsorption. According to Wuana *et al.* (2009) many different oxygen-based acidic functional groups are present on the surface of activated carbon which includes carboxyl groups, phenolic hydroxyls, quinine-type carbonyls, lactones, carboxylic acid anhydrides, ethers and cyclic peroxides.

FT-IR analysis: The FT-IR spectra of the adsorbents are as presented in Fig. 3. CIG150 shows a weak but broad band at 2914.8 cm^{-1} (3,200 – 2,700 cm^{-1}) characteristic of O-H stretching vibration indicating intra-molecular bonding. While the bands at 1,636.3 and 1,401.5 cm^{-1} are attributable to C=C bending vibration due to conjugated alkene and O–H bending vibration due to carboxylic acid. The CIG300 spectrum has a broad but weak peak at 2,903.6 cm^{-1} (3200 – 2,700 cm^{-1}) attributable to O–H stretching vibration due to intra-molecular bonding as in CIG150. The weak absorption band at 2,195.4 cm^{-1} (2,260 – 2,190 cm^{-1}) could be ascribed to C≡C stretching vibration due to disubstituted alkyne. The strong band at 1,021.3 cm^{-1} (1,075 – 1,021 cm^{-1}) is characteristic of C–O stretching vibration. CAC on the other hand gave a spectrum with broad and weak absorption band at 3,164.5 cm^{-1} that could be ascribed to O-H stretching vibration due to intra-molecular bonding. Adsorption bands at 2,885.0 cm^{-1} (3000 – 2,840 cm^{-1}) and 2,109.7 cm^{-1} (2,140 – 2,100 cm^{-1}) could be ascribed to C – H and C≡C stretching vibrations due to alkanes and monosubstituted alkynes, respectively. The medium adsorption bands at 1,576.7 cm^{-1} (1,650 – 1,566 cm^{-1}) and 1,181.6 cm^{-1} are attributable to C=C and C – N stretching vibrations due to cyclic alkene and amine respectively. Finally, the strong absorption band at 670.9cm^{-1} could be assigned to C=C bending vibration (730 – 665 cm^{-1}) or C – Br stretching vibration (690 – 515 cm^{-1}). In general, the FT-IR spectra of the adsorbents indicate that the adsorption of phosphate ions onto the adsorbents was via hydroxyl, carboxylic and amine, groups (Akl *et al.*, 2014; Wuana *et al.*, 2016; Maulina and Iriansyah, 2018).
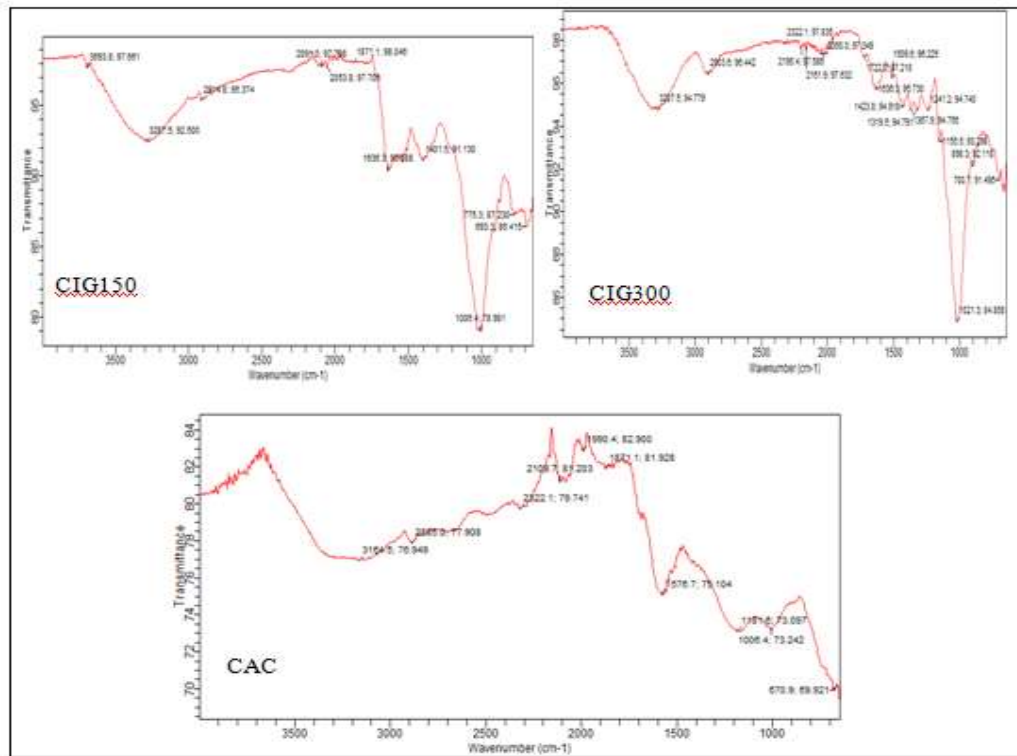
FUW Trends in Science & Technology Journal, www.ftstjournal.com
e-ISSN: 24085162; p-ISSN: 20485170; April, 2021: Vol. 6 No. 1 pp. 024 – 037

028

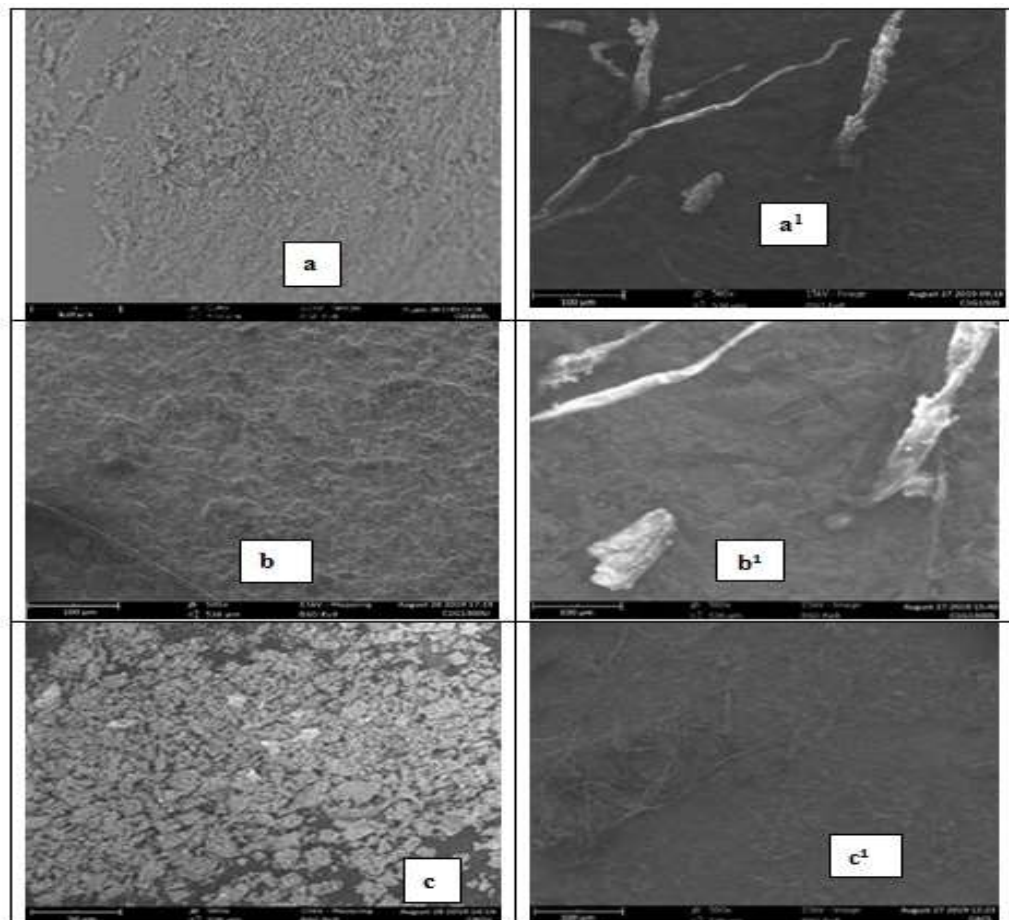**Fig. 3: Fourier transform infrared (FT-IR) spectra of CIG150, CIG300 and CAC**

Fig. 4: SEM micrographs of *Irvingia gabonensis* seed shells carbon (CIG150 = 150 μm; CIG300 = 300 μm particle size) and commercial activated carbon (CAC), (a) for unused CIG150, (a¹) for spent CIG150 (b) for unused CIG300, (b¹) for spent CIG300, (c) for unused CAC and (c¹) for spent CAC

FUW Trends in Science & Technology Journal, www.ftstjournal.com
e-ISSN: 24085162; p-ISSN: 20485170; April, 2021: Vol. 6 No. 1 pp. 024 – 037

029

Scanning electron analysis: The scanning electron micrographs of the unused and spent adsorbents are as presented in Fig. 4. The micrographs of the unused CIG150, CIG300 and CAC indicate that all the adsorbents were more dominated with micropores as compared to the mesopores. However, the pore structure of CIG150 and CAC were more regular as compared with that of CIG300. On the other hand, the pore structure of the spent adsorbents indicated a shrinked porosity with channel deposits on the surface for CIG150 and CIG300, while that of spent CAC was polished. These micrographs suggest that pore diffusion will be the sole rate limiting step during adsorption of phosphate ions on all the activated carbons. Furthermore, the dominance of micropores on the adsorbents also suggests that small-sized contaminants would be preferentially adsorbed. The micrographs generally show irregular structure and heterogeneous surface morphology with varieties of pores. The irregular surface may be attributed to a complex network of pores due to the action of the activating reagent on the botanical structure altering the surface morphology of the adsorbents (Maulina and Iriansyah, 2018; Akl *et al.*, 2014; Zhang *et al.*, 2014).

Anions and cations present in the wastewater
The following anions and cations were identified through qualitative tests and found to be present in the wastewater collected from the a multipurpose chemistry laboratory: Cl^-, SO_4^{2-}, NO_3^-, PO_4^{3-}, CO_3^{2-}, Pb^{2+}, Cu^{2+}, Ni^{2+}, Zn^{2+}, Mn^{2+}, Fe^{3+}. The results of this qualitative test yielded information that guided in the selection of phosphate ions for the study.

Effect of initial solution pH on adsorption of phosphate ions from wastewater
The plot in Fig. 5 illustrates the effect of initial solution pH on the removal of phosphate ions in wastewater from a multipurpose chemistry laboratory using activated carbon derived from seed shells of *I. gabonensis* and a commercial activated carbon.

The adsorption capacity of adsorbents is influenced mostly by the solution pH, since solution pH affects adsorbent's charge, degree of ionization and speciation of the adsorbate (Bernal *et al.*, 2017). The effect of initial solution pH on the aqueous phase sorptive removal of phosphate ions in wastewater generated from an advanced multipurpose chemistry laboratory by CIG150, CIG300 and CAC were demonstrated. At pH value of 3, phosphate ions adsorption in terms of adsorption capacity and removal efficiency [mg/g (% removal)] were respectively 0.473 (17.02), 0.533 (19.15) and 0.651 (23.40) for CIG150, CIG300 and CAC, respectively. As pH was increased, the maximum adsorption capacity/removal efficiency [mg/g (% removal)] of 1.420 (51.06), 1.538 (55.32) and 1.598 (57.45) were achieved for CIG150, CIG300 and CAC at pH 7. Further increase in the initial solution pH led to a decrease in the adsorption capacity/efficiency. The

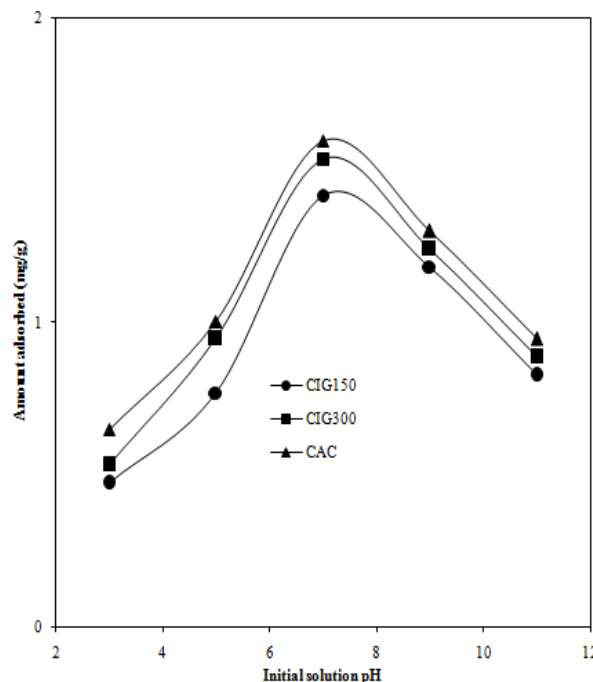potency/efficiency of these adsorbents for the removal of phosphate ions were in the order of CAC>CIG300>CIG150.

Fig. 5: Effect of initial solution pH on removal of phosphate ions from wastewater by *I. gabonensis* seed shells carbon (CIG150 = 150 µm; CIG300 = 300 µm particle size) and commercial activated carbon (CAC)

Effect of adsorbent dosage on adsorption of phosphate ions from wastewater
Figure 6 illustrates the effect of adsorbent dosage on the removal of phosphate ions in wastewater from a multipurpose chemistry laboratory using activated carbon derived from seed shells of *I. gabonensis* and a commercial activated carbon.
As reflected in Fig. 6, the uptake of phosphate per unit mass of adsorbent (CIG150, CIG300 and CAC) decreased with increase in the adsorbent dosage for all adsorbents at all the temperatures. This may be explained on the basis of mass balance relationship (Equation 6). The initial solution concentration is fixed as well as volume of solution, the available phosphate molecules are not enough to cover all the active adsorption sites on the adsorbents as adsorbent dosage is increased, resulting in low phosphate uptake. These results are in agreement with works reported by Akl *et al.* (2014) and Wuana *et al.* (2016).
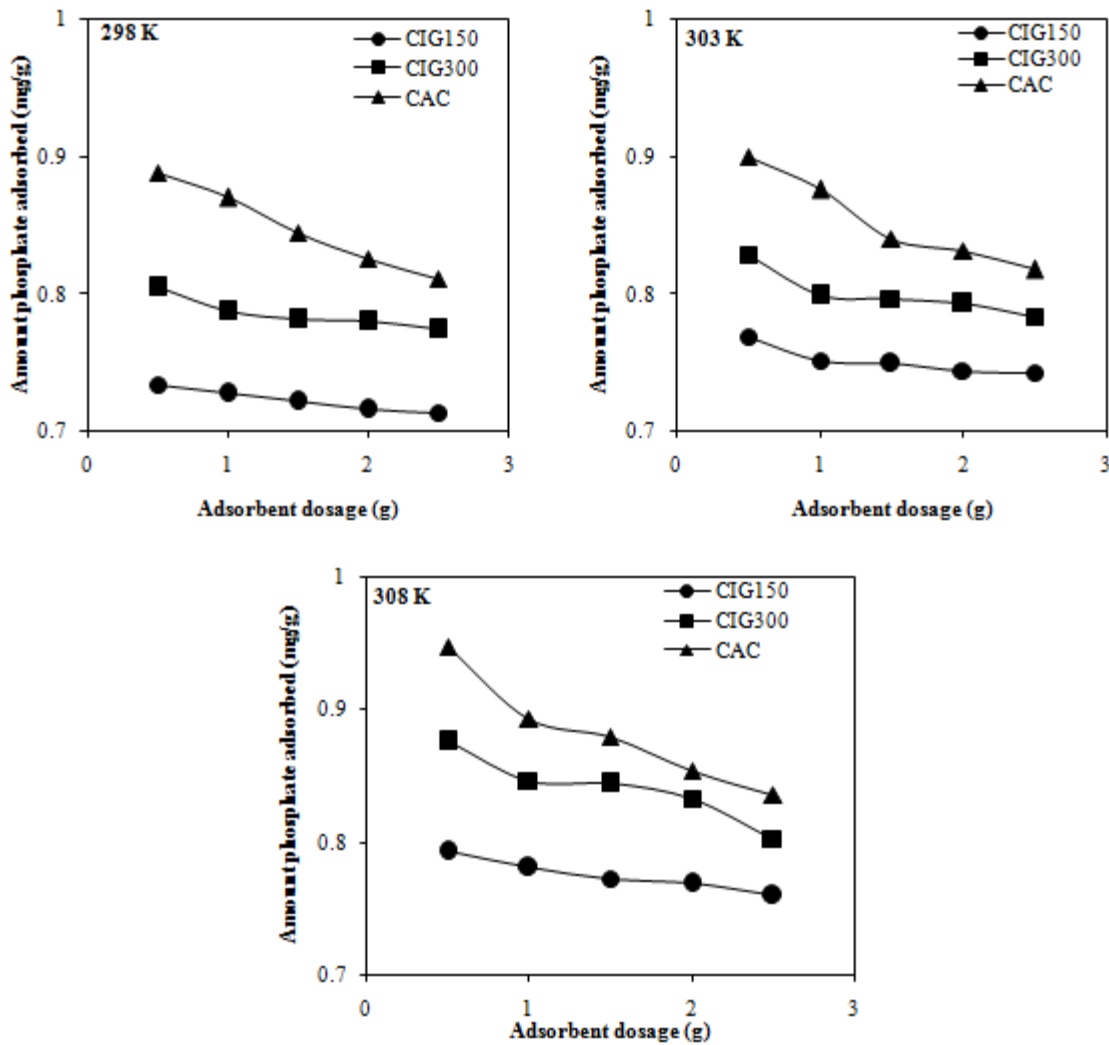
FUW Trends in Science & Technology Journal, www.ftstjournal.com
e-ISSN: 24085162; p-ISSN: 20485170; April, 2021: Vol. 6 No. 1 pp. 024 – 037

030

Fig. 6: Effect of adsorbent dosage on phosphate removal from wastewater *by I. gabonensis* seed shells carbon (CIG150 = 150 µm; CIG300 = 300 µm particle size) and commercial activated carbon (CAC) at different temperatures

Langmuir isotherm models for adsorption of phosphate ions

Figures 7 – 9 illustrate the linearized Langmuir isotherms for the removal of phosphate ions in wastewater from a multipurpose chemistry laboratory using activated carbon derived from seed shells of *Irvingia gabonensis* and a commercial activated carbon at different temperatures. The Langmuir Isotherm parameters are as presented in Table 2.

The isotherm profiles are important given that, information regarding the nature and mechanism of adsorption for a particular adsorbate-adsorbent system are revealed. Equilibrium data from adsorption experiments are usually presented in the form of an isotherm, which graphically displays the ratio of sorbed to non-sorbed solute per unit mass of the adsorbent at constant temperature (Wuana *et al*., 2016). Equilibrium data for the adsorption of phosphate from the wastewater onto CIG150, CIG300 and CAC were fitted into the linearized forms of the Langmuir, Freundlich, Temkin and Dubinin-Radushkevich models and only the Langmuir Isotherm fitted well as presented in Figs. 7 – 9.
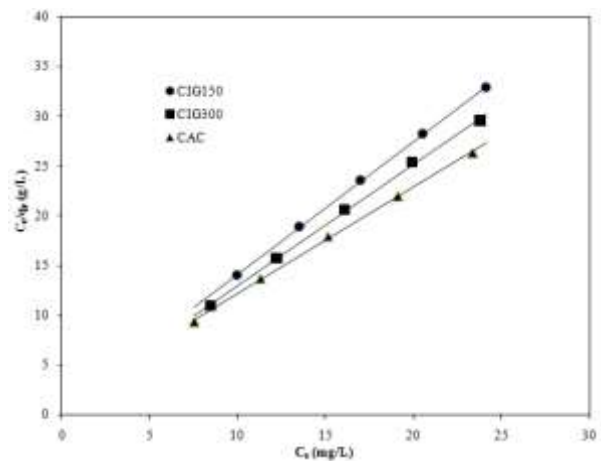

Fig. 7: Linearized Langmuir isotherms for adsorption of phosphate ions from wastewater by *I. gabonensis* seed shells carbon (CIG150 = 150 µm; CIG300 = 300 µm particle size) and commercial activated carbon (CAC) at 298K
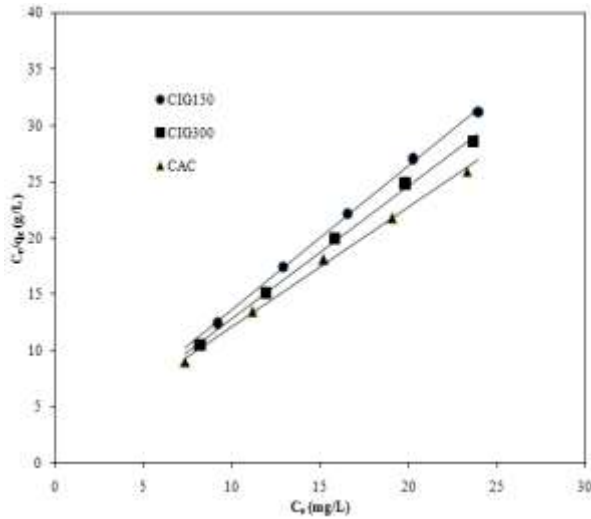
FUW Trends in Science & Technology Journal, www.ftstjournal.com
e-ISSN: 24085162; p-ISSN: 20485170; April, 2021: Vol. 6 No. 1 pp. 024 – 037
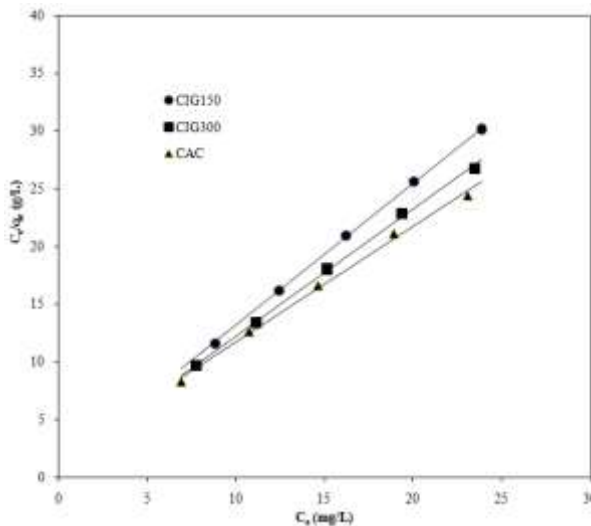
031

Fig. 8: Linearized Langmuir Isotherms for Adsorption of Phosphate ions from Wastewater by *I. gabonensis* Seed Shells Carbon (CIG150 = 150 µm; CIG300 = 300 µm Particle Size) and Commercial Activated Carbon (CAC) at 303K

Fig. 9: Linearized Langmuir isotherms for adsorption of phosphate ions from wastewater by *I. gabonensis* seed shells carbon (CIG150 = 150 µm; CIG300 = 300 µm particle size) and commercial activated carbon (CAC) at 308K
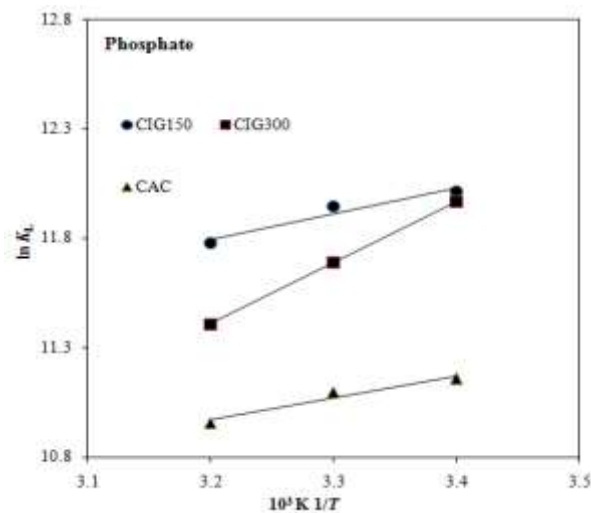

Fig. 10: Van't Hoff plot for aqueous phase removal of phosphate ions

The Langmuir model assumes that adsorption occurs at homogeneous sites and forms a monolayer. In this study, the Langmuir parameters considered at temperatures ranging from 298 K to 308 K were Q_m (maximum adsorption capacity corresponding to a monolayer coverage on the adsorbent surface in mg/g), K_L (the Langmuir constant in L/mol) and R_L (a dimensionless equilibrium parameter called separation factor used to indicate the nature of adsorption to be either unfavourable, linear, favourable or irreversible. From the results in Table 2, the maximum adsorption capacity, Q_m, for all the adsorbate-adsorbent systems increased with increasing temperatures. For the phosphate-adsorbent systems, Q_m values were high indicating the potency of the adsorbents in the order of CAC>CIG300>CIG150 at all temperatures. The values of R_L were all within $0<R_L<1$ range for all the adsorbents, signifying favourable adsorption (Wuana *et al*., 2016).

Thermodynamics of adsorption of phosphate ions
Thermodynamic parameters such as Gibbs free energy change (ΔG^o), enthalpy change (ΔH^o) and entropy (ΔS^o) were calculated using the following equations as described by Wuana *et al*. (2016). The Gibbs free energy change was calculated using:

$$\Delta G^o = -RT \ln K_L \qquad (16)$$

Where R is the universal gas constant (8.314 J/mol.K), T is the temperature (K). Meanwhile, the values of K_L, the Langmuir affinity constant, were first converted from L/mg basis to L/mol basis with the aid of Eq. 17 before substitution in Eq. 16:

$$K_L (L/mol) = K_L (L/mg) \times 10^3 (mg/g) \times f_w (g/mol) \quad (17)$$

Where f_w is the formula weight of phosphate ions (94.97136 g/mol)

The enthalpy (ΔH^o) and entropy (ΔS^o) parameters were respectively estimated from the slope and intercept of the ln K_L (L/mol) versus $(10^3$ K)/T plots shown in Fig. 10 from the Van't Hoff equation:

$$\ln K_L = \frac{\Delta S^o}{R} - \frac{\Delta H^o}{RT} \qquad (18)$$

Where R and T retain their meaning as defined in Eq. 16. Some thermodynamic parameters for aqueous phase removal of the phosphate ions by CIG150, CIG300 and CAC are summarized in Table 3.

Table 3: Some thermodynamic parameters for adsorption of phosphate by *I. gabonensis* seed shells carbon (CIG150 = 150 µm; CIG300 = 300 µm particle size) and commercial activated carbon (CAC) at different temperatures

Adsorbent	T (K)	ΔG^o (kJ mol^{-1})	ΔH^o (kJ mol^{-1})	ΔS^o (JK^{-1}mol^{-1})
Phosphate–CIG150			-9.7265	66.9327
	298	-29.761		
	303	-30.086		
	308	-30.161		
Phosphate–CIG300			-23.2568	20.4267
	298	-29.211		
	303	-29.448		
	308	-29.649		
Phosphate – CAC			-8.3398	65.5100
	298	-27.641		
	303	-27.953		
	308	-28.055		

FUW Trends in Science & Technology Journal, www.ftstjournal.com
e-ISSN: 24085162; p-ISSN: 20485170; April, 2021: Vol. 6 No. 1 pp. 024 – 037

032

The negative values of Gibbs free energy change *(ΔGᵒ)* for the adsorption of phosphate ions onto CIG150, CIG300 and CAC indicate that the adsorption process is spontaneous in nature (Das *et al.*, 2014). In general, the negative values of ΔG^o decreased with increase in temperature, indicating that the spontaneous nature of adsorption is inversely proportional to the temperature (Bulut and Tez, 2007). This trend of results observed is similar to that reported by (Piccin *et al.*, 2011). According to Wuana *et al*. (2015), ΔG^o values in the range of $-20.00 \leq \Delta G^o$ (kJ/mol) ≤ 0.00 represent physisorption, while those in the range of $-400.00 \leq \Delta G^o$ (kJ/mol) ≤ -80.00 indicate chemisorption. The ΔG^o values of this study are indicative of physical adsorption.

The negative values of enthalpy change (ΔH^o) i.e. -1.4948, -19.3150 and -3.8111 kJmol⁻¹ for phosphate-CIG150, phosphate-CIG300 and phosphate-CAC sorptive systems can be attributed to the exothermic nature of the adsorption process. The magnitude of enthalpy values give an idea about the type of sorption as enthalpy change values range of $2.1 \leq \Delta H^o$ (kJmol⁻¹) ≤ 20.9 signifies physical adsorption while $80 \leq \Delta H^o$ (kJmol⁻¹) ≤ 200 kJmol⁻¹ implies chemical adsorption (Saha and Chowdhury, 2011; Wuana *et al*., 2015). From the results obtained, the adsorption of phosphate ions onto CIG150, CIG300 and CAC are characteristic of physical adsorption.

The entropy change (ΔS^o) for the phosphate-CIG150, phosphate-CIG300 and phosphate-CAC sorptive systems are all positive indicating spontaneous nature of the adsorption of phosphate ions onto the adsorbents. These results reflect the affinity of the adsorbents towards phosphate ions and also suggest increased randomness at the solid-liquid interface with some structural changes in the adsorbates/adsorbents (Saha and Chowdhury, 2011; Wuana *et al*., 2015).

Adsorption kinetics

Adsorption rate curves: The plots in Fig. 11 illustrates rate curves for the removal of phosphate ions in wastewater from a multipurpose chemistry laboratory using activated carbon derived from seed shells of *I. gabonensis* and a commercial activated carbon at different temperatures.

From the rate curves for the adsorption of phosphate ions onto CIG150, CIG300 and CAC, the adsorption capacity generally increased with time throughout the time range under study (i.e. 10 – 240 min). However, for all the phosphate-adsorbent sorption systems, the uptake of the phosphate ions increased very rapidly in the first 10 min and then slowed down leading to marginal increase in the uptake of the phosphate ions. Based on the adsorption capacities of the adsorbents as depicted in Fig. 11, the adsorption efficiency/potency of the adsorbents was in the order of CAC>CIG300>CIG150 at all the temperatures studied.
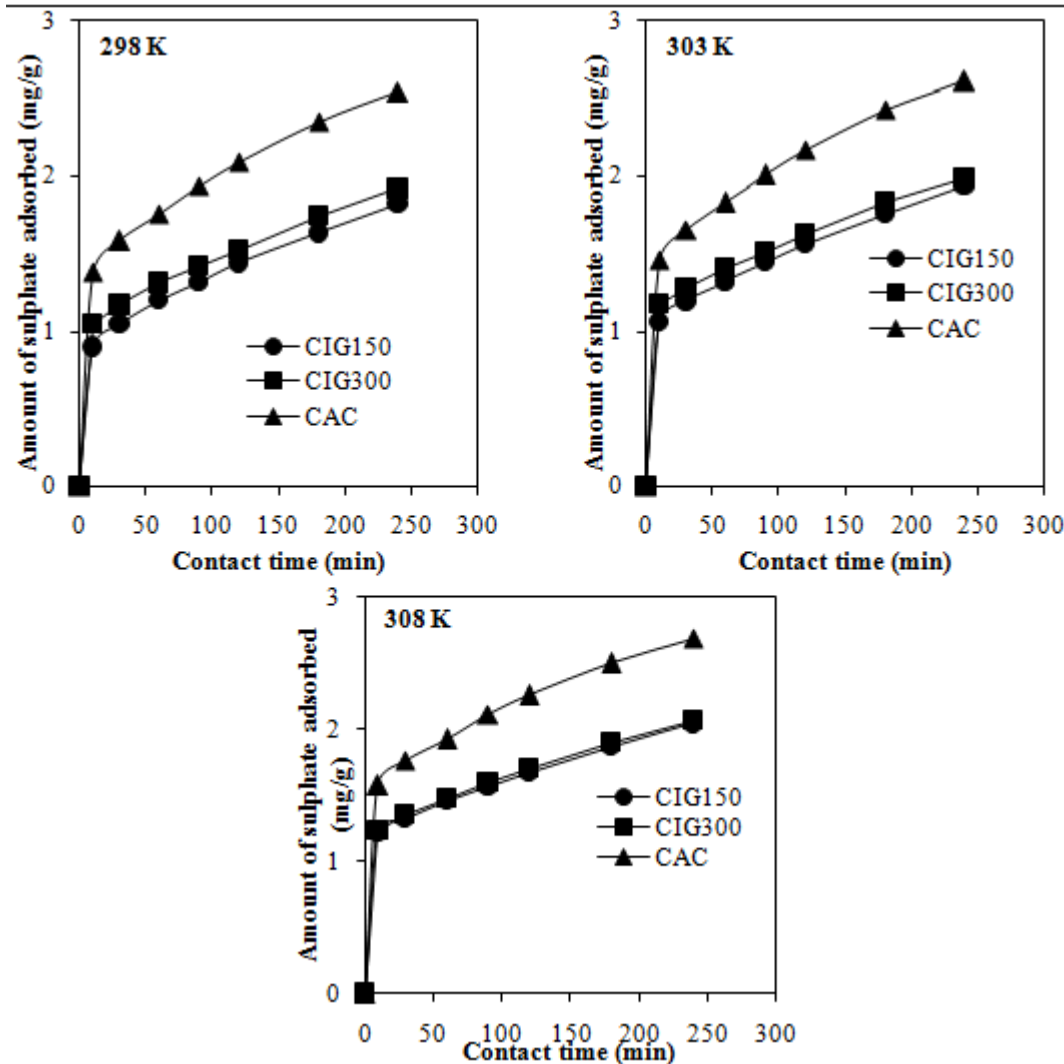

Fig. 11 Rate curves for removal of phosphate from wastewater by *I. gabonensis* seed shells carbon (CIG150 = 150 μm; CIG300 = 300 μm particle size) and commercial activated carbon (CAC)

FUW Trends in Science & Technology Journal, www.ftstjournal.com
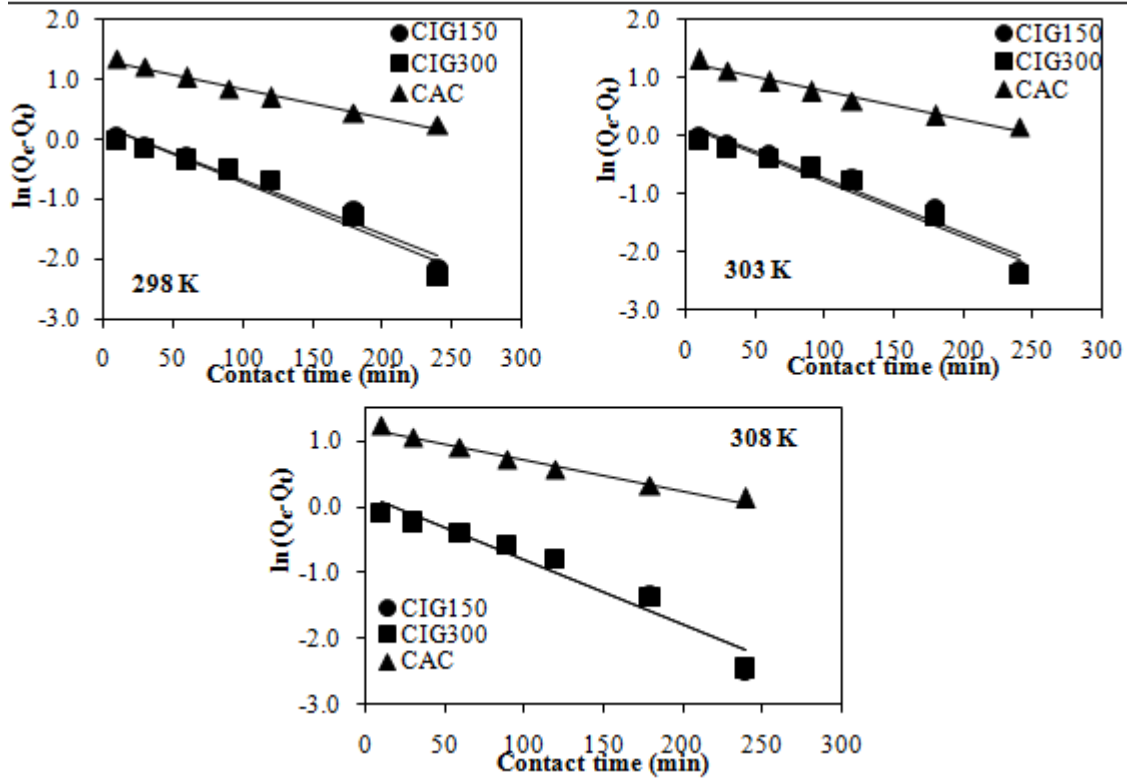**e-ISSN: 24085162; p-ISSN: 20485170; April, 2021: Vol. 6 No. 1 pp. 024 – 037**

033

Fig. 12: Lagergren pseudo-first order kinetic plots for removal of phosphate from wastewater by *I. gabonensis* seed shells carbon (CIG150 = 150 μm; CIG300 = 300 μm particle size) and commercial activated carbon (CAC)
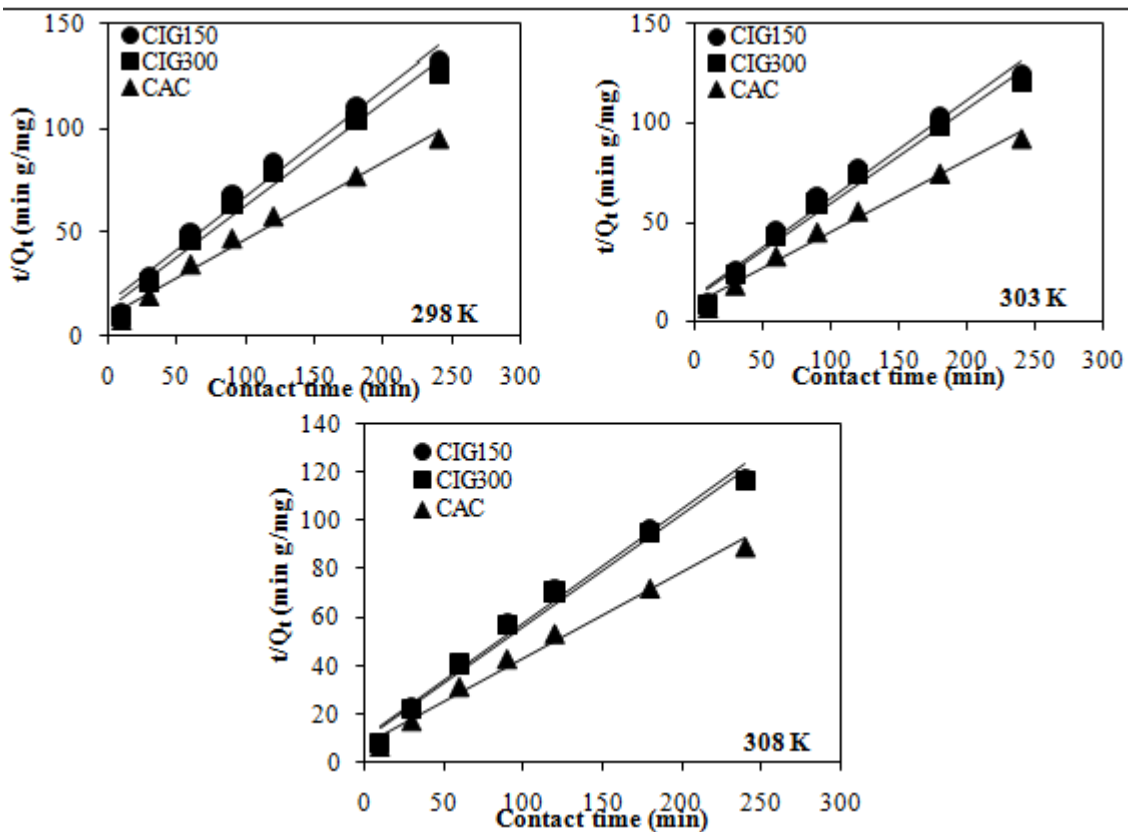

Fig. 13: Blanchard pseudo-second order kinetic plots for removal of phosphate from wastewater by *I. gabonensis* seed shells carbon (CIG150 = 150 μm; CIG300 = 300 μm particle size) and commercial activated carbon (CAC)

FUW Trends in Science & Technology Journal, www.ftstjournal.com
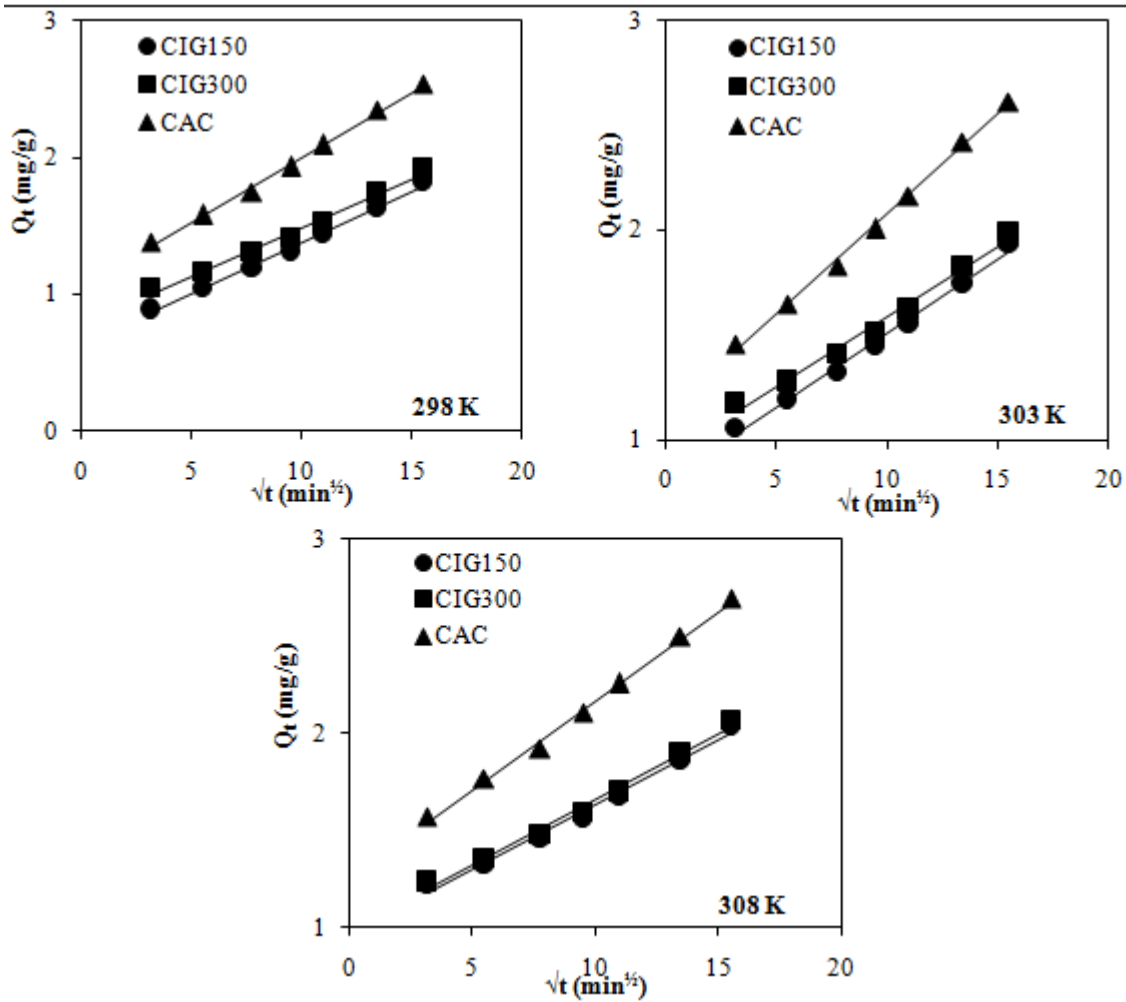**e-ISSN: 24085162; p-ISSN: 20485170; April, 2021: Vol. 6 No. 1 pp. 024 – 037**

034

Fig. 14: Weber-Morris intra-particle diffusion plots for removal of phosphate from wastewater by *I. gabonensis* seed shells carbon (CIG150 = 150 μm; CIG300 = 300 μm particle size) and commercial activated carbon (CAC)

Adsorption kinetic models: The experimental data for the sorptive removal of phosphate ions in wastewater from an advanced multipurpose chemistry laboratory by CIG150, CIG300 and CAC as a function of contact time were fitted into the linear forms of Lagergren pseudo-first-order, Blanchard pseudo-second order and Weber-Morris intra-particle diffusion kinetic models as presented in Figs. 12 – 14 and the kinetic parameters summarized in Table 4. The phosphate-CIG150 sorption system recorded ranges of the kinetic parameters across the temperatures as $9.0 \leq k_1 (\times 10^{-3}) \leq 9.8$, $17.6 \leq k_2 (\times 10^{-3}) \leq 21.6$, $67.0 \leq k_{id} (\times 10^{-3}) \leq 74.4$. In a similar fashion, the phosphate-CIG300 sorption system recorded the kinetic parameters in the order of $9.3 \leq k_1 (\times 10^{-3}) \leq 9.7$, $19.1 \leq k_2 (\times 10^{-3}) \leq 21.8$, $67.0 \leq k_{id} (\times 10^{-3}) \leq 70.8$ while the phosphate-CAC sorption system recorded $4.8 \leq k_1 (\times 10^{-3}) \leq 4.9$, $15.3 \leq k_2 (\times 10^{-3}) \leq 16.6$, $91.8 \leq k_{id} (\times 10^{-3}) \leq 95.3$. It is however worthy to note that the magnitude of the kinetic parameters for the phosphate-adsorbent sorption systems were in the order of $k_1 (\times 10^{-3}) < k_2 (\times 10^{-2}) \approx k_{id} (\times 10^{-2})$. The experimental values of k_1 did not follow a regular pattern for all the sorption systems, perhaps the kinetic data was not well modelled by the Lagergren pseudo-first-order model, while k_2 however increased with increasing temperature for the Blanchard pseudo-second-order model. Conversely, k_{id} values for the Weber-Morris intra-particle diffusion model decreased with increasing temperature (Das *et al.*, 2014; Wuana *et al.*, 2015; Wuana *et al.*, 2016).

Table 4: Kinetic parameters for adsorption of selected anions on carbonized *Irvingia gabonensis* seed shells (CIG150 and CIG300) and commercial adsorbent (CAC) at different temperatures

Adsorbent	Kinetic model	298 K	303 K	308 K
CIG150	Lagergren - k_1 (min^{-1})	0.0090	0.0094	0.0098
	R^2	0.9594	0.9481	0.9399
	Blanchard - k_2 (g.mg^{-1}min^{-1})	0.0176	0.0196	0.0216
	R^2	0.9782	0.9818	0.9849
	Weber-Morris: k_{id}(mg.g^{-1}min$^{-1/2}$)	0.0744	0.0708	0.0670
	R^2	0.9960	0.9928	0.9877
CIG300	Lagergren - k_1 (min^{-1})	0.0093	0.0095	0.0097
	R^2	0.9496	0.9500	0.9468
	Blanchard - k_2 (g.mg^{-1}min^{-1})	0.0191	0.0212	0.0218
	R^2	0.9799	0.9840	0.9857
	Weber-Morris: k_{id}(mg.g^{-1}min$^{-1/2}$)	0.0708	0.0675	0.0670
	R^2	0.9892	0.9865	0.9899
CAC	Lagergren - k_1 (min^{-1})	0.0048	0.0049	0.0048
	R^2	0.9814	0.9757	0.9767
	Blanchard - k_2 (g.mg^{-1}min^{-1})	0.0153	0.0155	0.0166
	R^2	0.9856	0.9863	0.9880
	Weber-Morris: k_{id}(mg.g^{-1}min$^{-1/2}$)	0.0953	0.0951	0.0918
	R^2	0.9970	0.9969	0.9960

FUW Trends in Science & Technology Journal, www.ftstjournal.com
e-ISSN: 24085162; p-ISSN: 20485170; April, 2021: Vol. 6 No. 1 pp. 024 – 037

035

On the basis of coefficient of determination, R^2, Weber-Morris intra-particle kinetic model recorded the highest values relative to Lagergren pseudo-first-order and Blanchard pseudo-second-order kinetic models. This indicates that the adsorption kinetics was better interpreted by the Weber-Morris intra-particle kinetic model (Wuana *et al*., 2016). But on the contrary, the linear plots of the Weber-Morris intra-particle kinetic model did not pass through the origin. According to Das *et al*. (2014), this kind of deviation from the origin can be explained on the basis of difference in the rate of mass transfer in the initial and final stages of the sorption process. This observation indicates the existence of some boundary layer effect and also showed that Weber-Morris intra-particle kinetic model is not the sole rate determining mechanism in the sorption process.

Conclusion

The synthesized adsorbents (CIG150 and CIG300) exhibited good physicochemical attributes which are comparable to the commercial adsorbent (CAC) and thus suggest preferential adsorption of small-sized contaminants with pore diffusion as the rate limiting step in the adsorption of phosphate ions. A good number of anions and cations were present in the laboratory wastewater collected for the study including chloride, sulphate, nitrate, phosphate, carbonate, lead (II), copper (II), nickel (II), zinc (II), manganese (II) and iron (III) ions. This identification test provided the information necessary for the selection of phosphate ions for the study.

The optimum pH for the uptake of phosphate ions onto CIG150, CIG300 and CAC was found to be 7. The adsorption capacity for the uptake of phosphate ions in wastewater from an advanced chemistry laboratory onto the adsorbents under study was found to decrease with increase in the adsorbent dosage. Only Langmuir isotherm model fitted well the equilibrium data for the uptake of phosphate ions onto CIG150, CIG300 and CAC indicating that the adsorption occurs at homogeneous sites and forms a monolayer. The maximum adsorption capacity was found to increase with increasing temperature.

From the thermodynamic point of view, the uptake of phosphate ions onto CIG150, CIG300 and CAC was found to be spontaneous in nature but the spontaneity was inversely proportional to the temperature. It was also found that the uptake of phosphate ions was characteristic of physical adsorption and exothermic in nature. The kinetic data fitted the Weber-Morris intra-particle diffusion model better than either Lagergren pseudo-first-order model or Blanchard pseudo-second-order model; although it was found that intra-particle diffusion was not the sole rate determining mechanism. All the adsorbents exhibited good efficiency/potency for the uptake of phosphate ions and their maximum adsorption capacities show that their potency was in the order of CAC>CIG300>CIG150 and could be incorporated in water treatment plants in place of high cost activated carbon.

Conflict of Interest

Authors declare that there is no conflict of interest reported in this work.

References

Abia AA & Asuquo ED 2007. Kinetics of Cd (II) and Cr (III) sorption from aqueous solutions using mercaptoacetic acid modified and unmodified oil palm fruit fibre (Elaeis guineensis) adsorbents. *Tsinghua Sci. and Techn.*, 12(4): 485–492.

Aderemi AO & Falade TC 2012. Environmental and health concerns associated with the open dumping of municipal solid waste: a Lagos, Nigeria experience. *Amer. J. Envtal. Engr.*, 2(6): 160–165. https://doi.org/10.5923/j.ajee.20120206.03

Agrawal S, Jain D & Sarkar S 2015. Hybrid adsorbent for selective recovery of phosphorus from contaminated water. In *Int. Conf. on Innov. in Chem. and Agric. Engr. (ICICAE'2015) Feb. 8-9, 2015* (pp. 8–11). Kuala Lumpur (Malaysia).

Akinjare OA, Ayedun CO, Oluwatobi AO & Iroham OC 2011a. Impact of sanitary landfills on urban residential property value in Lagos State, Nigeria. *J. Sust. Devt.*, 4(2): 48–60. https://doi.org/10.5539/jsd.v4n2p48

Akinjare OA, Oloyede SA, Ayedun CA & Oloke OC 2011b. Price effects of landfills on residential housing in Lagos, Nigeria. *Int. J. Marketing Studies*, 3(2): 64–72. https://doi.org/10.5539/ijms.v3n2p64

Akl AM & Nidà SM 2012. Biosorption of copper (II) and lead (II) ions from aqueous solutions by modified loquat (Eriobotrya japonica) leaves (MLL). *J. Chem. Engr. and Materials Sci.*, 3(1): 7–17. https://doi.org/10.5897/JCEMS11.061

Akl AM, Dawy MB & Serage AA 2014. Efficient removal of phenol from water samples using sugarcane bagasse based activated carbon. *J. Anal. and Bioanal. Techniques*, 5(2): 189. https://doi.org/10.4172/2155-9872.1000189

Al-Qahtani KM 2016. Water purification using different waste fruit cortexes for the removal of heavy metals. *J. Taibah Uni. for Sci.*, 10(5): 700–708. https://doi.org/10.1016/j.jtusci.2015.09.001

Alghanmi SI, Al-Sulami A, El-Zayat TA, Alhogbi BG & Salama MA (2015). Acid leaching of heavy metals from contaminated soil collected from Jeddah, Saudi Arabia: kinetic and thermodynamic studies. *Int. Soil and Water Res.*, 3: 196–208.

Ameh PO, Odoh R & Oluwaseye A 2012. Equilibrium study on the adsorption of Zn (II) and Pb (II) ions from aqueous solution onto *Vitex doniana* nut. *Int. J. Modern Chem.*, 3(2): 82–97.

Aminu AS, Gimba CE, Kagbu J, Turoti M, Itodo AU & Sarigya AI 2010. Sorption efficiency study of pesticide adsorption on granulated activated carbon from groundnut shell using GC/MS. *World Rural Observations*, 2(1): 18–24.

Bernal V, Erto A, Giraldo L & Carlos Moreno-Pirajan J 2017. Effect of solution pH on the adsorption of paracetamol on chemically modified activated carbons. *Molecules*, 22(27): 1032. https://doi.org/10.3390/molecules22071032

Bulut Y & Tez Z 2007. Removal of heavy metals from aqueous solution by sawdust adsorption. *J. Envtal. Sci.*, 19(2): 160–166.

Cardenas-Peña AM, Ibanez JG & Vasquez-Medrano R 2012. Determination of the point of zero charge for electrocoagulation precipitates from an iron anode. *Int. J. Electrochem. Sci.*, 7: 6142–6153.

Chislock MF, Doster E, Zitomer RA & Wilson AE 2013. Eutrophication: causes, consequences, and controls in aquatic ecosystems. *Nature Education Knowledge*, 4(4): 10.

FUW Trends in Science & Technology Journal, www.ftstjournal.com
e-ISSN: 24085162; p-ISSN: 20485170; April, 2021: Vol. 6 No. 1 pp. 024 – 037

036

Dada AO, Olalekan AP, Olatunya AM & Dada O 2012. Langmuir, Freundlich, Temkin and Dubinin-Radushkevich isotherms studies of equilibrium sorption of Zn^{2+} unto phosphoric acid modified rice husk. *IOSR J. Appl. Chem.*, 3(1): 38–45.

Das B, Mondal NK, Bhaumik R & Roy P 2014. Insight into adsorption equilibrium, kinetics and thermodynamics of lead onto alluvial soil. *Int. J. Sci. and Techn.*, 11: 1101–1114. https://doi.org/10.1007/s13762-013-0279-z

Fasoto T, Arawande J & Akinnusotu A 2014. Adsorption of zinc and chromium ions from aqueous solution onto sugarcane bagasse. *Int. J. Modern Chem.*, 6(1): 28–47.

Fu F & Wang Q 2011. Removal of heavy metal ions from wastewaters: a review. *J. Envtal. Mgt.*, 92(3): 407-418.

Geurts JJM, Sarneel JM, Willers BJC, Roelofs JGM, Verhoeven JTA & Lamers LPM 2009. Interacting effects of sulphate pollution, sulphide toxicity and eutrophication on vegetation development in fens: A mesocosm experiment. *Environmental Pollution*, 157: 2072–2081. https://doi.org/10.1016/j.envpol.2009.02.024

Gusau BU 1992. *Practical Chemistry for Senior Secondary School Students*. Ibadan: NPS Educational Publishers Limited.

Hanchar DW 1991. *Effects of Septic-tank Effluent on Ground-water Quality in Northern Williamson County and southern Davidson County*. Tennessee. Retrieved from http://pubs.usgs.gov/wri/wri914011/pdf/wrir_91-4011_a.pdf

Harvey D 2000. *Modern Analytical chemistry* (1st ed.). New York: McGraw-Hill Companies Inc.

Hassan LG, Ajana BN, Umar KJ, Sahabi DM, Itodo AU & Uba A 2012. Comparative batch and column evaluation of thermal and wet oxidative regeneration of commercial activated carbon exhausted with synthetic dye. *Nig. J. Basic and Appl. Sci.*, 20(2): 93–104.

Itodo AU & Itodo HU 2010. Sorption energies estimation using Dubinin-Radushkevich and Temkin adsorption isotherms. *Life Science Journal*, 7(4): 31–39.

Khalil AH, Alquuzweeni SS & Modhloom HM 2015. Removal of Copper Ions from Contaminated Soil by Enhanced Soil Washing. *Int. J. Envtal. Res.*, 9(4): 1141–1146.

Mallikarjun SD & Mise SR 2012. A study of phosphate adsorption characteristics on different soils. *IOSR Journal of Engineering*, 2(7): 13–23.

Maulina S & Iriansyah M 2018. Characteristics of activated carbon resulted from pyrolysis of the oil palm fronds powder. In: *IOP Conference Series: Materials Science and Engineering* 309. IOP Publishing Ltd. https://doi.org/10.1088/1757-899X/309/1/012072

Namasivayam C & Sangeetha D 2005. Removal and recovery of nitrate from water by $ZnCl_2$ activated carbon from coconut coir pith, an agricultural solid waste. *Indian J. Chem. Techn.*, 12: 513–521.

Oboh, I. O., Aluyor, E. O., and Audu, T. O. K. (2013). Second-order kinetic model for the adsorption of divalent metal ions on Sida acuta leaves. *Int. J. Physical Sci.*, 8(34): 1722–1728. https://doi.org/10.5897/IJPS09.146

Okiemen FE, Okiemen CO & Wuana RA 2007. Preparation and characterization of activated carbon from rice husks. *J. Chem. Soc. Nig.*, 32(1): 126–136.

Oladapo MI, Adeoye-Oladapo OO & Adebobuyi FS 2013. Geoelectric study of major landfills in the Lagos metropolitan area, southwestern Nigeria. *Int. J. Water Resources and Envtal. Engr.*, 5(7): 387–398. https://doi.org/10.5897/IJWREE12.020

Olorunfemi FB 2009. Living with waste: major sources of worries and concerns about landfills in Lagos metropolis, Nigeria. *Ethiopian J. Envtal. Stu. and Mgt.*, 2(2): 12–19.

Olorunfemi FB 2011. Landfill development and current practices in Lagos metropolis, Nigeria Landfill development in Lagos State. *J. Geogr. and Reg. Plan.*, 4(12): 656–663.

Paul I, Egu SA & Ocholi SS 2016. Aqueous phase removal of ciprofloxacin using adsorbents from Moringa oleifera pod biomass; kinetics studies. *Int. Adva. J. Nat. and Appl. Sci.*, 1(1): 1–9.

Piccin JS, Dotto GL & Pinto LAA 2011. Adsorption isotherms and thermochemical data of FDandC RED N° 40 Binding by chitosan. *Brazilian J. Chem. Engr.*, 28(2): 295–304. https://doi.org/10.1590/S0104-66322011000200014

Saha P & Chowdhury S 2011. Insight Into Adsorption Thermodynamics. In: *Thermodynamics 2,* Tadashi M. (Ed.), InTech, Rijeka-Croatia, pp. 350–363.

Stoica L, Jitaru L & Radu N 1999. Removal and recovery of phosphate from wastewater by floatation technique. *Phosphorus Research Bulletin*, 10: 466–474. https://doi.org/10.3363/prb1992.10.0_466

Utange PI, Wuana RA & Akpoghol TV 2015. Potentiometric and spectrophotometric determination of phosphoric acid in some beverages. *Der Chemica Sinica*, 6(3): 93–99.

Vrijheid M 2000. Health effects of residence near hazardous waste landfill sites: A review of epidemiologic literature. *Environmental Health Perspectives*, 108(1): 101–112.

WTEL (Water Technology Engineering Limited) 2016. Soakaway, Septic Tank Drainage, Drainfield installation. Retrieved May 19, 2016, from http://www.wte-ltd.co.uk/soakaways.html

WHO (World Health Organization) 2011. *Guidelines for Drinking-water Quality* (4th ed.). Malta: World Health Organization.

Wuana RA, Okiemen FE & Imborvungu JA 2010. Removal of heavy metals from a contaminated soil using organic chelating acids. *Int. J. Environ. Sci. Tech.*, 7(3): 485–496.

Wuana, R. A., Sha'Ato, R., and Iorhen, S. (2015). Aqueous phase removal of ofloxacin using adsorbents from Moringa oleifera pod husks. *Advances in Environmental Research*, 4(1), 49–68.

Wuana RA, Sha'Ato R & Iorhen S 2016. Preparation, characterization, and evaluation of Moringa oleifera pod husk adsorbents for aqueous phase removal of norfloxacin. *Desalination and Water Treatment*, 57: 11904–11916. https://doi.org/10.1080/19443994.2015.1046150

Ye H, Zhang L, Zhang B, Wu G & Du D 2012. Adsorptive removal of Cu (II) from aqueous solution using modified rice husk. *Int. J. Engr. Res. and Applic.*, 2(2): 855–863.

Yoder C 2016. Qualitative Analysis. Retrieved October 3, 2016, from http://www.wiredchemist.com/chemistry/instructional/laboratory-tutorials/qualitative-analysis

Zhang Y, Zhao J, Jiang Z, Shan D & Lu Y 2014. Biosorption of Fe (II) and Mn (II) ions from aqueous solution by rice husk ash. *BioMed Res. Int.*, 1–10. https://doi.org/10.1155/2014/973095

FUW Trends in Science & Technology Journal, www.ftstjournal.com
e-ISSN: 24085162; p-ISSN: 20485170; April, 2021: Vol. 6 No. 1 pp. 024 – 037

037